

## SEPARATING SURFACE MAGNETIC EFFECTS IN SUNSPOT SEISMOLOGY: NEW TIME-DISTANCE HELIOSEISMIC DIAGNOSTICS

S.P. RAJAGURU<sup>1</sup>

W.W. Hansen Experimental Physics Laboratory, Stanford University, Stanford CA 94305

*Draft version January 9, 2019*

### ABSTRACT

Time-distance helioseismic measurements in surface- and deep-focus geometries for wave-paths that distinguish surface magnetic contributions from those due to deeper perturbations beneath a large sunspot are presented and analysed. Travel times showing an increased wave speed region extending down to about 18 Mm beneath the spot are detected in deep-focus geometry that largely avoids use of wave field within the spot. Direction (in- or out-going wave) and surface magnetic field (or focus depth) dependent changes in frequency dependence of travel times are shown and identified to be signatures of wave absorption and conversion in near surface layers rather than that of shallowness of sunspot induced perturbations.

*Subject headings:* Sun: helioseismology — Sun: magnetic fields — Sun: oscillations — sunspots

### 1. INTRODUCTION

A problem of major importance in solar and stellar magnetohydrodynamics is the determination of sub-surface magnetic and thermal constitution of sunspots (Thomas & Weiss 1992). Application of time-distance helioseismology (Duvall et al. 1993) in 3-d tomographic imaging of subsurface layers of sunspots (Duvall et al. 1996; Kosovichev & Duvall 1999; Zhao et al. 2001, 2006) provided a major milestone in the seismology of sunspots (Thomas et al. 1982, 1988). Continuing developments in local helioseismology, notably helioseismic holography accompanied by theoretical modelling, have since identified several "surface" contributors to seismic measures, collectively known as "surface magnetic effects" (Braun 1997; Schunker et al. 2005; Lindsey & Braun 2005a,b; Zhao et al. 2006), that arise from interactions of p modes with surface magnetic field of a sunspot. However, such interactions have so far not been explicitly included in helioseismic inversions, for lack of a suitable model, and hence relative contributions of surface and sub-surface perturbations have so far not been estimated.

Use of oscillation signals observed within sunspots is known to be the primary source of most surface effects in sunspot seismology (Braun 1997; Lindsey 2006), as well as the associated observational errors (Rajaguru et al. 2007) and systematics in the analysis procedure (Rajaguru et al. 2006). In this Letter, using waves with a first skip travel distance sufficiently larger than the diameter of sunspot under study, and employing deep-focus wave-path geometries that largely avoid wavefield observed within the sunspot, we present new time-distance helioseismic diagnostics that contrasts near-surface perturbations with deeper ones. Signatures of a deep (up to about a depth of 18 Mm) increased wave speed region, obtained using waves in deep-focus geometry are presented in Section 3. Further support for this inference, from frequency dependences of surface- and

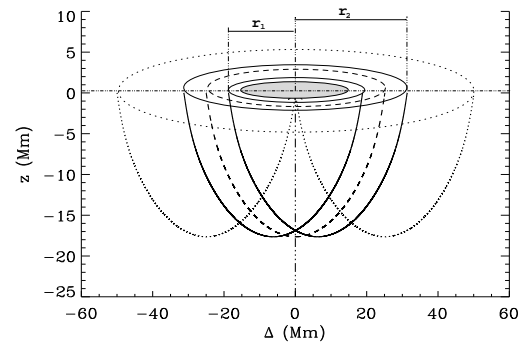


FIG. 1.— Ray-path diagram depicting the surface- and deep-focus measurement geometries: the ray paths correspond to model S of Christensen-Dalsgaard et al. (1996). Dotted lines correspond to the well-known center-annulus geometry, and solid and dashed lines correspond to annulus-annulus deep focus geometry with  $q=0.6$  and 1 (focus at the lower turning point), respectively

deep-focus travel times, are presented in Section 4.

### 2. DATA AND ANALYSIS METHOD

A large sunspot (NOAA AR9057, diameter  $\approx 32$  Mm) that crossed the central meridian on 28 June, 2000 and observed by SOHO/MDI (Scherrer et al. 1995) in the full-disk resolution mode has been chosen for this study. We extracted a data cube of size  $373 \text{ Mm}^2$  by 1024 minute and have also obtained vector magnetograms of the same region observed by IVM instrument at Hawaii (Hannah Schunker, private communication). The data were pre-processed through the Stanford data pipeline system to remap and track the region under study.

We choose waves having a first skip travel distance,  $\Delta$ , of 50 Mm that is larger than the diameter of the sunspot. Apart from a phase speed filter that selects waves with horizontal phase speed around 54 km/s with a width (FWHM) of 21.25 km/s, Gaussian frequency filters centered around 2.5, 3, 4 and 5 mHz with widths of 1 mHz are also used to study frequency dependences of travel times (Braun & Birch 2006). We employ three distinct measurement schemes (Figure 1): (i) the traditional center-annulus surface focus geometry (dotted

Electronic address: rajaguru@sun.stanford.edu

<sup>1</sup> Currently at: Indian Institute of Astrophysics, Bangalore - 560034, India

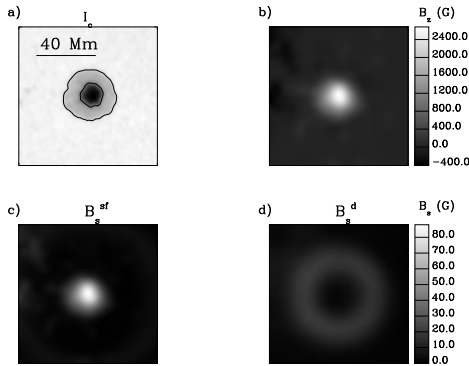


FIG. 2.— a). MDI continuum intensity ( $I_c$ ) image of the sunspot (contours mark the umbral and penumbral boundaries, b) smoothed, by a 3 pixel width Gaussian, IVM line of sight magnetogram rescaled to MDI resolution, c) and d) the reduced magnetograms  $B_s$  derived using Eqn.(1) for surface- and deep-focus (average of  $q=0.75, 0.8$  and 1 cases) geometries; see text for more details

lines), which, for the travel distance chosen, makes use of wave-field within sunspot either as a 'source' (out-going waves) or as a 'receiver' (in-going waves) but not both simultaneously, (ii) double skip center-annulus surface focus geometry, which completely avoids sunspot oscillation signals for measurements over a region of radius 43 Mm from the spot center, and (iii) an annulus-annulus deep focus geometry with focus depths,  $z_d$ , ranging from 10.24 - 17.65 Mm (solid and dashed lines correspond to  $z_d = 16.85$  and 17.65 Mm, respectively; details in Section 2.1).

Most studies have used the LOS magnetic field on the surface as a proxy for characterizing 'surface signal' in the seismic measures (Lindsey & Braun 2005a,b; Braun & Birch 2006). We note that, in the presence of a deep perturbation extending from the surface, surface magnetic field can be a proxy for neither the surface effects nor deeper perturbations in seismic signals individually and exclusively. Since a seismic quantity, either a wave travel time or phase, measured at any single location (pixel) uses wave field observed at distant points that are spread over an annulus or pupil, a more appropriate proxy to characterize the surface effect would be similarly averaged surface magnetograms: weighted convolution of pupil functions,  $a(x, y)$ , (or masks for 'center' and 'annulus' locations used to average the wave-field) with the magnetograms,  $B(x, y)$ , given by,

$$B_s(x, y) = \int a(x - x', y - y') B(x', y') w(r) dx' dy' \quad (1)$$

that gives each pixel a weighted average of surface magnetic field over all the pixels from where the wave-field used in a travel time measurement has come from (Figure 2). Weights,  $w(r)$ , for magnetic field at a given location  $(x', y')$  is chosen to be the inverse of its horizontal distance,  $r$ , from the focus point (the measurement point,  $x, y$ ), because the density of rays or wave-paths projected on to the surface go as inverse distance from the focus. We use such reduced or averaged magnetograms,  $B_s(x, y)$ , to study any direct surface magnetic field induced variations in travel times. The magnetic field  $B(x, y)$  used here are LOS field strengths obtained from IVM vector magnetograms rescaled to MDI full-disk

TABLE 1  
ANNULI RADII, FOCUS DEPTHS AND  $B_{su}$   
( $\Delta=50$  MM)

$r_1$ (Mm)	$r_2$ (Mm)	$z_d$ (Mm)	$B_{su}$ (G)
0.	$\Delta$	0.	60.0
6.25	43.75	10.24	43.0
10.0	40.0	13.12	29.0
12.5	37.5	14.53	20.0
18.75	31.25	16.85	6.5
21.43	28.57	17.35	4.0
22.22	27.78	17.45	3.7
25.0	25.0	17.65	3.0

resolution.

### 2.1. Deep-focus measurement scheme

Two concentric annuli, centered around the point of measurement, are used in our typical deep-focus measurement scheme, similar to the original scheme proposed by (Duvall et al. 2001): a point from the inner annulus is cross-correlated with a diametrically opposite point in the outer annulus, and all such point-to-point correlations spanning the whole annuli (360 degrees) are averaged. In this scheme, the travel distance  $\Delta = r_1 + r_2$ , where  $r_1$  and  $r_2$  are the radii of inner and outer annuli, respectively; and, different focus depths are achieved by varying the ratio  $q = r_1/r_2$  from 0 to 1, while keeping  $\Delta$  fixed;  $q = 0$  is the traditional surface focus, and  $q = 1$  is deep focus at the lower turning point. This latter case measurements were first performed by Duvall et al. (2001). Here, we perform 8 different focus depth measurements for the chosen  $\Delta = 50$  Mm, including the surface focus; Table 1 provides focus depths  $z_d$ , for the chosen  $r_1$  and  $r_2$ , computed using ray theory for standard solar model (model S of Christensen-Dalsgaard et al. (1996)) and corresponding umbral averages  $B_{su} = \langle B_s \rangle_{umbra}$ .

For deep focus measurements over the entire area of sunspot to be completely free of wave-field within the sunspot, both  $r_1$  and  $r_2$  should be greater than diameter of the sunspot, i.e.  $\Delta$  should be greater than 64 Mm; but changes in travel times of waves with such large  $\Delta$ , as measured in local methods, are too small to analyse the effects under study. Here, with  $\Delta = 50$  Mm, we aim at getting at least the measurements within umbral area to be free of wave-field within the sunspot, i.e.  $r_1$  and  $r_2$  should at least be the sum of umbral (5.8 Mm) and full sunspot radii (16 Mm). From Table 1, we see that the last 3 (deeper most) annuli combinations roughly satisfy such a criterion (see also Figure 2).

### 3. SEPARATING SURFACE EFFECTS: DEEP-FOCUS MEASUREMENTS

In deep focus geometry, contribution of oscillation signals from within the sunspot to a given measurement, as characterized by  $B_s$ , decreases as the focus depth increases; passage to  $B_s \approx 0$  G (Table 1 and Figure 2) occurs mainly in the umbral region, and so we study the variation of umbral averaged travel times against,  $B_{su}$ , the umbral averaged  $B_s$  (umbral area is marked by the inner contour in Figure 2a, and it is about 5.8 Mm in radius). Figure 3 shows the variation of changes, with respect to a quiet Sun average, in umbral averages of

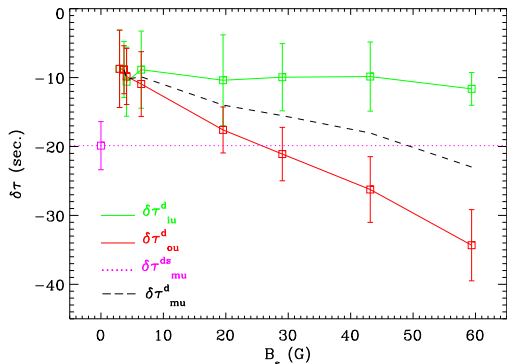


FIG. 3.— Variation of umbral area averaged one way and mean travel times against  $B_{su}$  for surface- and deep-focus geometries; see text for details.

one way (in- and out-going) and mean travel times,  $\delta\tau_{iu}^d$ ,  $\delta\tau_{ou}^d$  and  $\delta\tau_{mu}^d$ , against  $B_{su}$ . The error bars correspond to standard deviations of travel times over the umbral pixels. Surface-focus geometry yields a value of  $B_{su} = 60$  G, and the corresponding travel times  $\delta\tau_{iu}^s$  and  $\delta\tau_{ou}^s$  are the two right most data points in Figure 3. Umbral average of half of double skip travel times,  $\delta\tau_{mu}^{ds}$ , which have only a mean signal and are completely free of wave field within the sunspot (cf. Section 2) corresponding to a zero  $B_s$ , is given by the dotted horizontal line.

Several important pieces of information about the subsurface structure and interaction of p modes with the sunspot magnetic field are in order, in the variation of travel times against  $B_{su}$  shown in Figure 3, once we understand the variation of measurement geometry and dependent sensitivities to travel times. Firstly, because of geometry and the azimuthal averaging involved, the sensitivity to flows in deep focus measurements gradually decreases as  $z_d$  increases and is zero when  $z_d$  is the lower turning point for waves. This happens independent of  $B_s$ . On the other hand, passage towards  $B_{su} = 0$  G involves wave-paths changing from in and out of sunspot to that of crossing it at some depth. Because of the above reasons, the asymmetric variation of one way travel times to a non-zero mean value of  $\delta\tau_{mu}^d \approx -10$ . sec at  $B_{su} \approx 0$  G is accountable solely neither by material flow and its gradient in depth nor by effects localized near the surface due to predominant surface magnetic field interactions. An increased wave speed region extending down to, at least, a depth of about  $z_d - \lambda_h/2$ , where  $\lambda_h$  is the horizontal wavelength of waves with dominant power within the frequency band used, is essential here. For the model S of Christensen-Dalsgaard et al. (1996) the asymptotic relation (ray theory)  $\lambda_h = R_{\odot}c(r_t)/\nu r_t$  yields a value of about 15 Mm for frequency  $\nu=3.5$  mHz and lower turning point  $r_t=18$  Mm, and so the increased wave speed region should extend at least to within 7.5 Mm from the focus depth around 18 Mm. This is broadly in agreement with early time-distance helioseismic inversions for sound speed (Kosovichev & Duvall 1999), as far as the depth extent of positive sound speed changes is concerned. Secondly, attributing the largely  $B_{su}$  independent (hence, focus depth independent) values for  $\delta\tau_{iu}^d$  ( $\approx -10$ . sec.) solely to seismic signals from flow and sound speed requires a following surprising coincidence: (down)flow and sound speed perturbations both

have negative depth gradients such that their signatures in  $\delta\tau_{iu}^d$  (ingoing waves travelling against the flow) exactly cancel out, while those in  $\delta\tau_{ou}^d$  (outgoing waves travelling with the flow) add up leading to the changes seen in Figure 3. Frequency dependences of  $\delta\tau_{iu}^s$ ,  $\delta\tau_{ou}^s$  and  $\delta\tau_{mu}^{ds}$ , shown and discussed in the next Section, however, argue against such a scenario. Moreover, we find that half the double skip travel time  $\delta\tau_{mu}^{ds}$  (-20. sec.) is closer to  $\delta\tau_{iu}^s$  (-11. sec) than to  $\delta\tau_{ou}^s$  (-35. sec), confirming the early findings of Braun (1997). This result, again, depends on wave frequency as shown in the next Section.

In summary, results in Figure 3 show that use of wave-field observed within magnetic regions with significant  $B_s$  leads to travel time measurements that cannot be explained solely in terms of seismic signals due to flows and sound speed. However, our measurements in the limit of  $B_{su} \approx 0$  G, where both surface magnetic and flow contributions go to zero, show a significant mean travel time signal indicating a faster wave speed region extending down to about 18 Mm with a resolution uncertainty of  $\lambda_h/2 \approx 7.5$  Mm.

#### 4. ASYMMETRIC FREQUENCY DEPENDENCES OF ONE WAY TRAVEL TIMES

Frequency dependence of mean travel times, over a sunspot region, was shown and interpreted by Braun & Birch (2006) as an indication of perturbations largely confined to a region not deeper than a few Mm. Here, we show in Figure 4 the umbral averages  $\delta\tau_{iu}^s$ ,  $\delta\tau_{ou}^s$ ,  $\delta\tau_{mu}^{ds}$  and the deep focus times  $\delta\tau_{mu}^d$  ( $B_s \approx 0$ ) against frequency;  $\delta\tau_{mu}^d$  ( $B_s \approx 0$ ) shown here are the ones averaged over the three deep most foci measurements (Table 1).

Two important results concerning the sunspot - p mode interactions and deep structure of sunspot perturbations are contained in the frequency variations shown in Figure 4. (1) There is a large asymmetry in the frequency dependences of  $\delta\tau_{iu}^s$  and  $\delta\tau_{ou}^s$ : dominant frequency dependence is seen only in  $\delta\tau_{iu}^s$ , while that in  $\delta\tau_{ou}^s$  is very small, for the chosen  $\Delta$  of 50 Mm. A shallow sunspot perturbation cannot introduce such a direction dependent frequency variation; moreover,  $\delta\tau_{mu}^d$  ( $B_s \approx 0$ ) are largely independent of frequency. So, reasoning in the same lines as Braun & Birch (2006) rather suggests a deeper extension for wave-speed perturbation, provided we identify an independent physical cause for the frequency dependence of  $\delta\tau_{iu}^s$ , which we do in case (2) below. We note that for  $\Delta$  smaller than the diameter of sunspot, as is mostly the case in Braun & Birch (2006), and also from our results not discussed here, both  $\delta\tau_{iu}^s$  and  $\delta\tau_{ou}^s$  are equally frequency dependent. The asymmetric frequency dependence at larger  $\Delta$ , then, is likely due to 'source' and 'receiver' locations being outside or inside, but not both together within the spot: whenever waves from outside the spot are 'received' inside, there is a large frequency dependence but no or little frequency dependence vice versa. (2) The mean times  $\delta\tau_{mu}^{ds}$ , which correspond to waves with both 'sources' and 'receivers' being outside but focussing at a first skip surface location within the spot, are not only closer to  $\delta\tau_{iu}^s$ , but also have the same frequency dependence. This points to an intimate connection, helioseismically, between ingoing waves that survive the interaction with the sunspot to emerge on the other side and those 'observed' or 'received' within the sunspot: we interpret this as a helioseismic signature

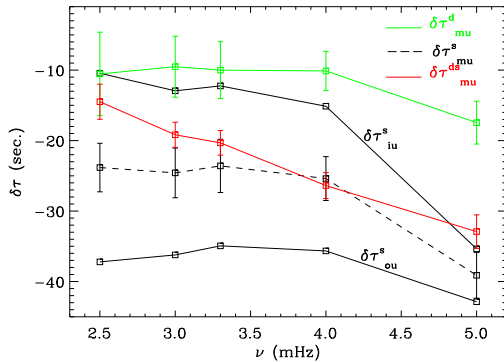


FIG. 4.— Frequency dependences of surface- and deep-focus travel times (one way and mean). Labels for different line types and colors identify the different measurements. For clarity, only error bars for mean travel times in surface focus (dashed line) measurement are drawn.

of well observed p mode absorption of sunspots. Further, as evident in Figure 4, the lower the frequency the smaller is the difference between  $\delta\tau_{mu}^{ds}$  and  $\delta\tau_{mu}^{su}$ . This might indicate that mode conversion is more efficient at lower frequencies, for a given phase speed, than at higher frequencies or to a wave-number dependent sunspot - p mode interaction.

## 5. DISCUSSIONS AND SUMMARY

Reliable three dimensional tomographic imaging of the whole depth range of sub-surface layers of a sunspot is hard to achieve without having to use waves skipping at distances smaller than the size of a sunspot and hence without explicitly taking into account the magnetic field - p mode interactions. Since we lack a suitable model for such interactions and it has been quite clear from various studies (Lindsey et al. (2007) and references therein) that significant seismic contributions arise due to surface magnetic field interactions, physical, instrumental and systematic, most sunspot local seismic inversions have suffered from unreliable depth discrimination of flow and

sound speed structures. Here, we have attempted a completely helioseismic diagnostic approach to checking the extent of surface magnetic effects by way of combining of surface- and deep-focus time-distance helioseismic measurements that avoid oscillation signals observed within the sunspot. Using an appropriate surface magnetic field proxy,  $B_s$ , derived from magnetograms, we have been able to contrast the near-surface perturbations with deeper ones.

Even though we have not proved that deep-focus measurements indeed have maximum sensitivities localized enough at the foci, with wave propagation calculations (which should form part of a future investigation), we believe that results presented in Sections 3 and 4 together provide strong observational evidences for an extended depth region of faster wave propagation beneath sunspots. Large asymmetry of one way travel times of waves focussing near the surface within a sunspot (i.e. when the surface magnetic field contribution is high) is also shown to be accompanied by asymmetric frequency dependence. We have identified such direction and surface magnetic field (or focus depth) dependent changes in frequency dependence of travel times to be helioseismic signatures of p mode absorption and mode conversion. The surface magnetic proxy  $B_s$  that we have defined in Eqn.(1) depends only on how oscillation signals on the surface are used in a given measurement and so should prove useful in characterizing 'surface magnetic' effects in different methods of local helioseismology.

This work was supported by NASA grants NNG05GH14G to *SOHO*/MDI project and NNG05GM85G to Living With a Star (LWS) program at Stanford University. The author thanks Dr. Sebastien Couvidat for a ray tracing computer code used in this work, and Dr. Richard Wachter for discussions that helped understanding the results in this paper better. Thanks are also due to Dr. Baba Verghese for help with Figure 1.

## REFERENCES

- Braun, D.C. 1997, ApJ, 487, 447  
 Braun, D.C., & Birch, C.A. 2006, ApJ, 647, L187  
 Braun, D.C., Lindsey, C., & Birch, A.C. 2004, BAAS, 204, 530  
 Christensen-Dalsgaard, J. et al. 1996, Science, 271, 1286  
 Duvall, T. L., Jr., D'Silva, S., Jefferies, S. M., Harvey, J. W., & Schou, J. 1996, Nature, 379, 235  
 Duvall, T. L., Jr., Jefferies, S. M., Harvey, J. W. & Pomerantz, M. A. 1993, Nature, 362, 430  
 Duvall, T. L., Jr., Jensen, J.M., Kosovichev, A.G. & Birch, A.C. 2001, American Geophysical Union, Spring Meeting 2001, Abstract No. SP22A-03  
 Kosovichev, A.G., Duvall, T.L., Jr., Scherrer, P.H. 2000, Sol. Phys., 192, 159  
 Kosovichev, A.G., & Duvall, T.L., Jr. 1999, Current Science, 77, 1467  
 Lindsey, C. 2006, Proc. of SOHO18/GONG2006/HELASI, Sheffield, UK (ESA SP-624)  
 Lindsey, C., & Braun, D.C. 2005a, ApJ, 620, 1107  
 Lindsey, C., & Braun, D.C. 2005b, ApJ, 620, 1118  
 Lindsey, C., Schunker, H., & Cally, P.S. 2007, Astronomische Nachrichten, 328, 298  
 Rajaguru, S.P., Birch, A.C., Duvall, T.L., Jr., Thompson, M.J., & Zhao, J. 2006, ApJ, 646, 543  
 Rajaguru, S.P., Sankarasubramanian, K., Wachter, R. & Scherrer, P.H. 2007, ApJ, 654, L175  
 Scherrer, P.H., et al. 1995, Sol. Phys., 162, 219  
 Schunker, H., Braun, D.C., Cally, P.S., & Lindsey, C. 2005, ApJ, 621, L149  
 Thomas, J.H., Cram, L.E., & Nye, A.H. 1982, Nature, 297, 485  
 Thomas, J.H., Lites, B.W., & Abdelatif, T.E. 1988, Adv. in Helio- and Asteroseismology, I.A.U. Symposium No. 123, p181  
 John H. Thomas & Nigel O. Weiss (eds.), Sunspots: theory and observations, NASA ASI series C: Mathematical and Physical Sciences, Kluwer Academic Publishers, Dordrecht, Vol.375  
 Zhao, J., Kosovichev, A.G., & Duvall, T.L., Jr. 2001, ApJ, 557, 384  
 Zhao, J., & Kosovichev, A.G. 2006, ApJ, 643, 1317